



# Modal-Displacement Based Design: Procedural aspects and application to a multi-storey Blockhaus structure

Martina Sciomenta<sup>a</sup>, Chiara Bedon<sup>b</sup>, Massimo Fragiacomò<sup>a</sup>, Yuri De Santis<sup>a</sup>,

<sup>a</sup> Department of Civil, Architecture and Building and Environmental Engineering, University of L'Aquila, Via Giovanni Gronchi 18, 67100 L'Aquila, Italy

<sup>b</sup> Department of Engineering and Architecture, University of Trieste, Via Alfonso Valerio, 6/1, 34127 Trieste, Italy

*Keywords: Displacement Based Design; Modal- Displacement Based Design; Seismic design on timber buildings; Blockhaus construction system*

## ABSTRACT

Under earthquake excitations, buildings undergo different levels of drift that can be associated with the damage both of structural and non-structural elements as well as with the expected losses. Therefore, in the Modal-DBD, identifying the interstory drift as a design criterion allows the designer to control the damage mechanism and the expected economic losses due to an earthquake. The extension to the design of timber buildings focused mainly on three DBD methods: DDBD, Modal-DBD and N2-DBD. The proposed Modal-DBD procedure is specifically designed for multi-storey wood structures with the aim of solving the drawbacks of current force-based procedures. In this work, innovation lies in the application of this methodology to a multi-storey timber building constructed using the Blockhaus technology. The backbone parameters have been obtained for each shearwall by FE analysis carried on with the software ABAQUS on the entire log-wall. Fundamental mechanisms for Blockhaus structure such as friction between logs, the presence of small gaps in corner joints and vertical compressive loads have been accounted in the solid FE model.

## 1 INTRODUCTION

In the last decades timber has become one of the most attractive and widespread construction material. It's diffusion is due to several reasons such as the sustainability, the lightness and hence excellent earthquake resistance, reduced cost of foundations, and ease of transport and erection (Fragiacomo et al. 2015). In the context of seismic performances, most of timber structures have been deeply analyzed (Foliente 1998). Although Blockhaus technology is one of the most ancient massive timber construction type, it's behaviour under lateral forces has been investigated only in the last years by testing (Branco and Araújo 2010) (Bedon, et al. 2014), or 3D numerical models (Bedon et al. 2015a) (Bedon et al. 2016), and dedicated studies for corner joints (Grossi et al. 2016) in order to find an analytical formulation (Sciomenta et al. 2018).

The goal of this paper is to investigate the possible application of Modal-DBD procedure to Blockhaus systems.

### 1.1 Displacement-based seismic design of buildings.

A seismic event induces on a structure as forces as well as displacements; traditionally, seismic design is based, above all, on the knowledge of the forces assigned to the structural elements, as it seems more consistent to relate them to the classical dead or gravity loads. On the other hand, it has been shown that displacements plays a key role when seismic actions occur. Force-Based Design, has been implemented in different Standards such as the current edition of International Building Code (ICC 2018), the seismic design provisions included in the ASCE 41-17 (2017) and Minimum Design Loads and Associated Criteria for Buildings and Other Structures, ASCE 7-16 (2016), suffers from several fundamental problems. The problems come upon the FBD approach are mainly

concerning the assumption of the initial elastic stiffness and the adoption of a specific force reduction factor to predict the inelastic behaviour.

Moreover the actual codified seismic design of structures is carried out with uniform-hazard spectrum for a fixed return period, leading to uncontrolled values of the failure probability, which vary with the structure and the location (Gkimprixis et al. 2019).

The DBD procedure is a multi-level design approach based on the displacement response spectrum as a cornerstone for calculating the base shear demand. Deformations or strains are, in fact, better quantities to assess the damage since the deformations are expected to go beyond the elastic values. The design procedure follows, as the FBD, the "Capacity Design" principles, i.e the "Hierarchy of Resistances" to ensure that the plastic hinges are formed only at pre-established points, obtaining a certain collapse mechanism.

To summarize, the DBD procedure has been carried out in order to overcome FBD limitations, allowing achievement of consistent performance levels for structures with different properties through the definition of uniform-risk design maps (Gkimprixis et al. 2019).

## 1.2 Main application to timber structures

Although several DBD procedures have been developed for different purposes in the last decades, in the framework of seismic design for a specified performance level of timber structures, the most consolidated methods are the Direct Displacement Based Design (DDBD) (Priestley et al. 2007), the Modal Displacement Based Design (Modal-DBD) (Pang and Rosowsky 2009). Whereas the N2 method (Fajfar and Gaspersic 1996) is the most widespread seismic evaluation procedure in Europe and the only one implemented in a Standard code: the EC8 (CEN 2004).

### 1.2.1 Direct- Displacement-based Design

The Direct Displacement-based Design (D-DBD) requires a little or no iteration to design structures that, for a given earthquake, respond with a specific limit displacement (defined in the codes), see (Priestley et al. 2007)

This method utilizes the secant stiffness  $K_e$  to maximum displacement  $\Delta_d$  based on the Substitute Structure (Priestley et al. 2007) and equivalent damping of a SDOF structure. The equivalent viscous damping  $\xi$  accounts for both the elastic damping and the hysteretic energy absorbed during inelastic response, thus, the material and type of structure, for a given level of ductility

demand, have different level of viscous damping (Priestley et al. 2007). The main difficulties are related to the definition of Substitute Structure parameters.

### 1.2.2 Modal- Displacement-based Design

The Modal Displacement-based Design (Modal-DBD) was proposed by Pang and Rosowsky (Pang and Rosowsky 2009) for designing multi-story light-frame wood buildings related to the NEESWood Project. The main feature of this procedure consists in performing a normalized modal analysis to define the displacement capacity of building, based on the basic hypothesis, that the stiffness of each panel is proportional to the relative length.

Displacement capacity and demand are expressed in terms of inter-story drift, fixed at the beginning. The key role is performed by the backbone load-displacement curves, necessary to estimate the parameters that will be employed to define the envelope response  $F_b(\delta)$ , and so the equivalent stiffness yield  $k_{el}$ . This method will be discussed deeply in Section 2.

### 1.2.3 N2 DBD-Method

The N2-DBD method was introduced by Fajfar and Gaspersic (Fajfar and Gaspersic 1996) for RC structures and has been incorporated into Annex B of EC8 (CEN 2004) (Loss et al. 2018). This model is suitable for the evaluation of seismic behaviour of buildings both existing as well as new, for which the fundamental mode is predominant. The name N2 imply the basic features of the method: 2 because the method is based on the use of two separate mathematical models, and N accounts for the application of the response spectrum approach and of the non-linear static analysis. Another fundamental hypothesis considers the choice of a damage model which includes cumulative damage (Fajfar and Gaspersic 1996).

## 2 MODAL-DBD METHOD

### 2.1 General Procedure

The procedure below has been developed for multistory wood-frame structures and requires as input data, the knowledge of the structural features (in order to perform the modal analysis and obtain the Backbone Curves development) and the definition of the inter-story drift limits for each performance level (i.e. IO, LS, CP).

The general steps for the multistory Modal DBD procedure, in accordance with (Pang and Rosowsky 2009) are represented in Figure 1:

1. Define multiple performances (inter-story drifts) for seismic hazard levels.
2. Calculate the mass and stiffness ratios (relative to first floor) for each floor.
3. Estimate inter-story drift factors and natural frequencies from normalized modal analysis on the MDOF system.
4. Construct inter-story drift spectra for the most severe hazard level and determine the required equivalent stiffness for each floor.
5. Select lateral force resisting system from wood shearwall design tables, which include information on shearwall backbone response and equivalent stiffness at various drift levels.
6. Check the design using the actual stiffness ratios (based on step 5). Revise the shearwall selection if necessary.
7. Repeat steps 2 - 6 for each performance level.
8. Compute design base shear, story shear and uplift force using the actual nonlinear backbone curves of shearwalls.

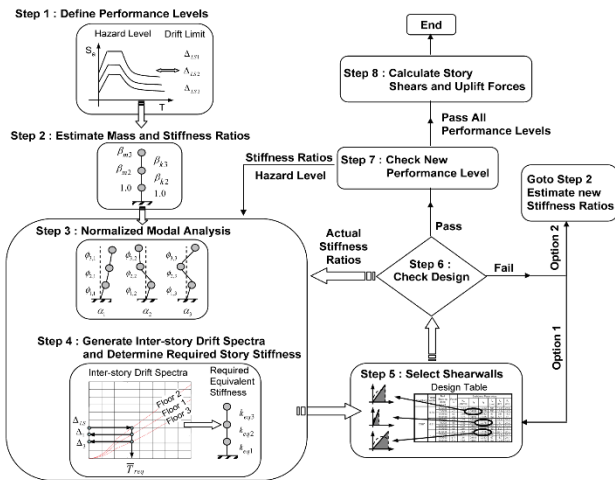


Figure 1. Flowchart for multi-story Modal-DBD procedure (Pang & Rosowsky, 2009)

## 2.2 Modal-DBD method applied to light-frame wood systems

As case study, Pang and Rosowsky took into account a 3-story light-frame structure, similar to the two-story benchmark structure of the CUREE-Caltech Woodframe project (Fischer et al. 2001).

The analyses were performed, placing the structure near City Hall in Los Angeles and California, and accounting for FEMA 356 provisions.

The procedure was based on design tables with shearwalls backbone parameters (calibrated for

walls with different types of connectors, nailing patterns and panel widths). The CASHEW program, along with available shear-wall test data, was used to generate the design tables (Pang and Rosowsky 2009).

## 2.3 Modal-DBD method applied to CLT system

The Modal-DBD method was adapted by Bovaldi et al. (Bolvardi et al. 2018) for isolated, 12-story CLT building in Los Angeles. The fundamental assumption assessed that most of the nonlinear displacement and energy dissipation will occur at the isolation layers and, when only one isolation layer is present, a multi-story system can be simplified into an equivalent 3-DOF system (equivalent segment below the isolation layer, isolation and upper equivalent segment). For each CLT story a monotonic push-over analysis was performed to identify the equivalent linear stiffness, mass and height for each of the stories in the CLT building. The validity of the process was verified by measuring the performance of the building through NLD analyses.

## 3 MODAL-DBD METHOD APPLIED TO BLOCKHAUS SYSTEM

### 3.1 An overview about the Blockhaus system

The Blockhaus log-walls are well known for having both partition and load-bearing features, so they perform a key role as lateral force resisting system in log-haus structures. In the last years, different authors have been carried out extensive monotone pushover (Figure 2) and the cyclic tests on corner joint specimens as well as on full-scale log-walls under lateral in-plane actions (Bedon, et al. 2015b), (Bedon, et al. 2015a), (Grossi et al. 2016) and (Branco and Araújo 2010). The friction phenomena, the mounting gaps and the corner joints are the main components that influence the in-plane response and led to a non-linear response. In particular, it is evident analyzing the log-wall and joints cyclic behavior, that:

- due to the friction phenomena, logs demonstrate a high level of energy dissipation,
- the vertical load defines the size of the hysteretic cycle,
- the local timber crushing due to compression perpendicular to the grain leads to a stiffness degradation for medium high displacement cycles.

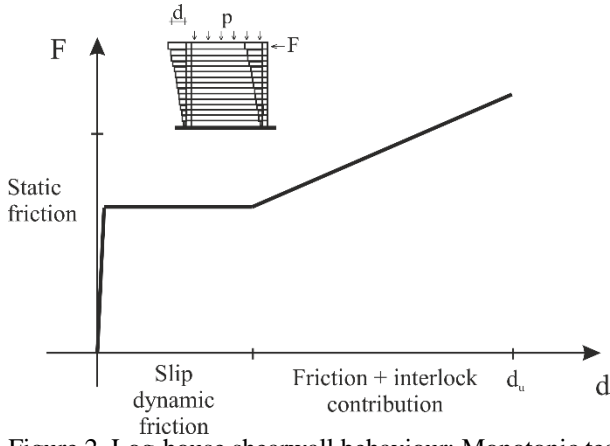


Figure 2. Log-house shearwall behaviour: Monotonic test

Due to the mentioned mechanisms, the cyclic behavior is characterized by pinching, stiffness and strength degradations. In the last decades, two hysteretic models have been developed (Beton, et al 2014) and (Grossi et al. 2016) both requiring, at least, the stiffness and the characteristics of a corner-joints.

### 3.2 Validation of the main hypothesis for the Modal- DBD application

#### 3.2.1 Log-wall stiffness proportional to length

The first assumption of Modal-DBD is considering the shearwall's stiffness proportional to the length. In order to verify this hypothesis, the formulation proposed in (Sciomenta et al. 2018) is considered:

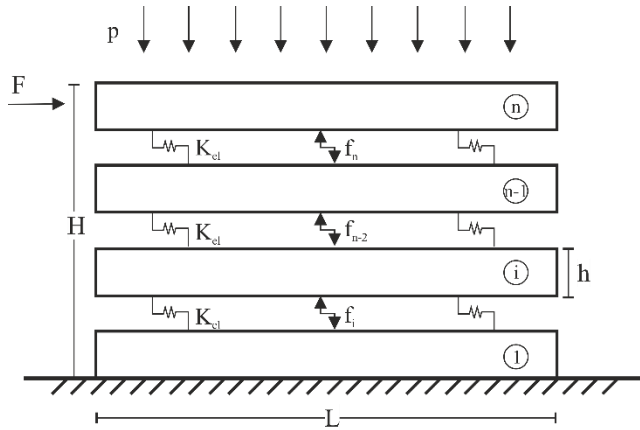


Figure 3. Log-house shear wall under combined in-plane compression and lateral loads: analytical model.

In Figure 3, the typical  $L \times H$  log-house shear wall is represented, by superposition of  $n$  logs in contact along their top-bottom surfaces, and a sill log joined at the foundation level. The foundation restraints are assumed indefinitely rigid. It is also assumed that the longitudinal logs interact with the orthogonal members by means of corner joints.

The main wall is then uniformly pre-compressed by a distributed load  $p$  and subjected to an in-plane lateral load  $F$ . Under the assigned load  $F$ , the top log displacement can be assumed

as the result of sequential relative displacements of logs, as well as of local mechanical behaviors (initial crushing in the region of notches, etc.), due to the progressive activation of the joints. The analytical model of Figure 3, in particular, assumes that the corner joints are represented in the form of linear elastic springs, with equivalent stiffness  $K_{el}$  (see in (Sciomenta et al. 2018)). The static friction effects are accounted, in the form of  $f$  Coulomb forces.

The presence of  $n$  tolerance gaps in the region of corner joints is also considered, as an additional contribution for the total displacement, where  $t_{gap}$  represents the gap amplitude (from 0.5 to 1mm). Given the structural system of Figure 3, possible internal joints and restraints are disregarded.

Neglecting the self-weight of logs, the friction contribution is:

$$f = \mu p L \quad (1)$$

where  $\mu$  is the static friction coefficient.

Assuming a vertical load  $p$  and corner joint stiffness  $K_{el}$ , the proportionality between the shear-wall stiffness and the wall length is:

$$K_{tot} = \frac{\mu p}{\delta_{top}} L + \frac{2 K_{el} \delta_i}{\delta_{top}} \quad (2)$$

where  $\delta_i$  represents the displacement of the  $i$ -th log each log, with  $i=2..n$ .  $\delta_{top}$  is the top displacement, that is::

$$\delta_{top} = n t_{gap} + \sum_{i=2}^n \delta_i \quad (3)$$

#### 3.2.2 CASHEW model implementation for Blockhaus structures

In order to evaluate the feasibility of Modal-DBD for Blockhaus structures, some similarities among Blockhaus and lightframe shear-walls are first highlighted. The Modal-DBD has been formulated based on the CASHEW model (Folz and Filiatrault 2001).

- a) Its basic hypothesis is that a shearwall deforms into a parallelogram when the top of the wall moves. The model is able to predict the load displacement response in the upper part of the wall by tracking the load-slip response of the connectors as well as the relative movements of shearwall components (sheathing panels and framing members). In Blockhaus, corner-joints act similarly to connectors in lightframe shear-walls.

In lightframe, the in-plane bending of the framing members (or studs) has a very

minor effect on the overall shearwall response (Gupta and Kuo 1985). The members of the frame can be modeled as rigid elements with pin-ended connections. The main source of lateral stiffness derives from the inelastic load-slip response of the sheathing-to-framing connectors. Similarly, the Blockhaus log-walls stiffness under lateral in-plane loads derives from corner-joints; preliminary studies highlighted that the individual logs shear deformation can be neglected, while the presence of hold-downs only prevent uplift.

### 3.3 Case of study introduction: a three-story Blockhaus structure

A three-story woodframe structure having plan dimensions of 5.64 m x 7.3 m and elevation views in Figures 4 to 7 was selected as an illustrative design example. The house layout (Figure 4 to 9) is similar to the Rusticasa structure from (SERIES 2013), with an additional storey equal to the second one. The height of the house increases from 6.88m at the edge to 8.00m at the ridge, forming a duo-pitch (gable) roof. Ground and first floor have both a height of 2.72m.

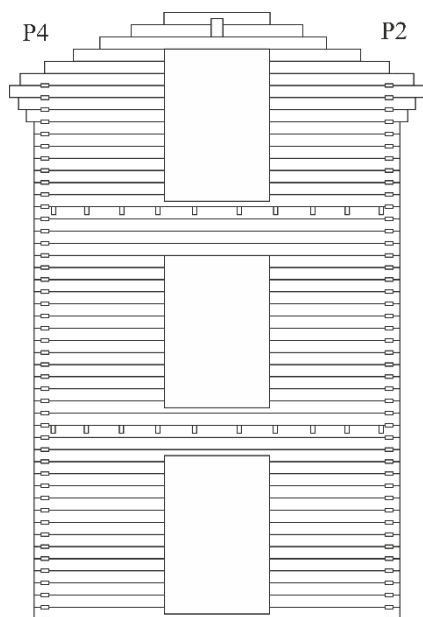


Figure 4. Wall P1 (West elevation, X-direction)

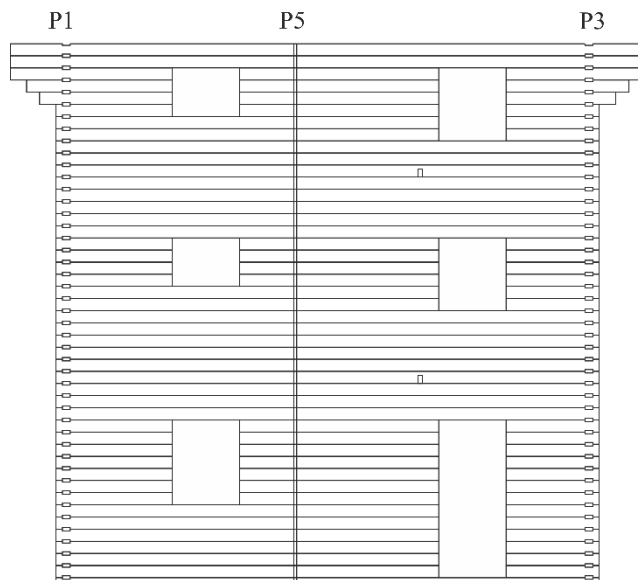


Figure 5. Walls P2 (North elevation, Y-direction) and P4

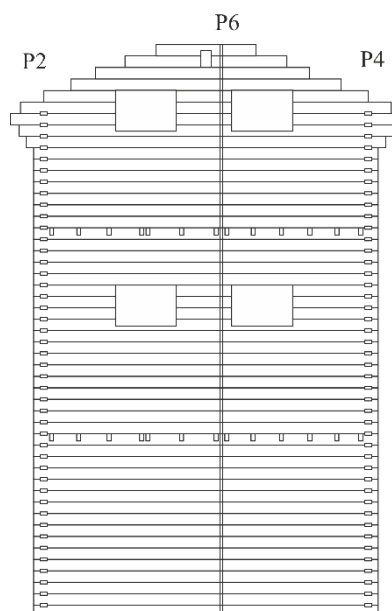


Figure 6. Wall P3 (East elevation, X-direction)

The plan of the structure is symmetrical in the longitudinal direction (Walls P2 and P4) and asymmetrical in the transverse direction (Walls P1 and P2). The floor beams are of size 90x165mm. In order to guarantee rigid in-plane behaviour of the diaphragm, the beams are superimposed by Oriented Strand Board (OSB) studded panels which are 22mm thick.

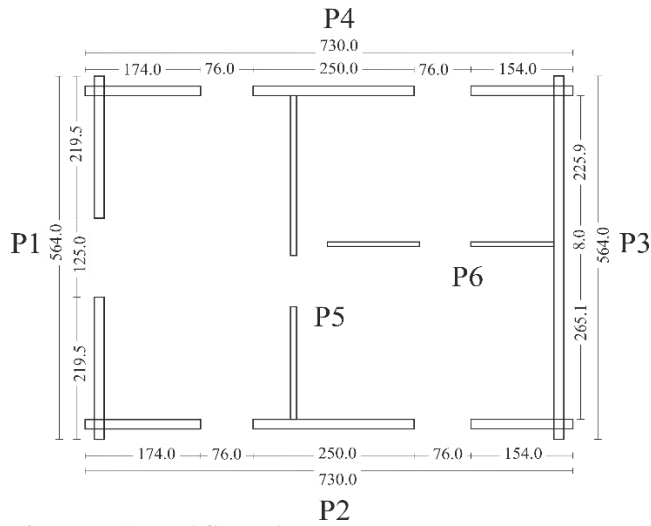


Figure 7. Ground floor plan

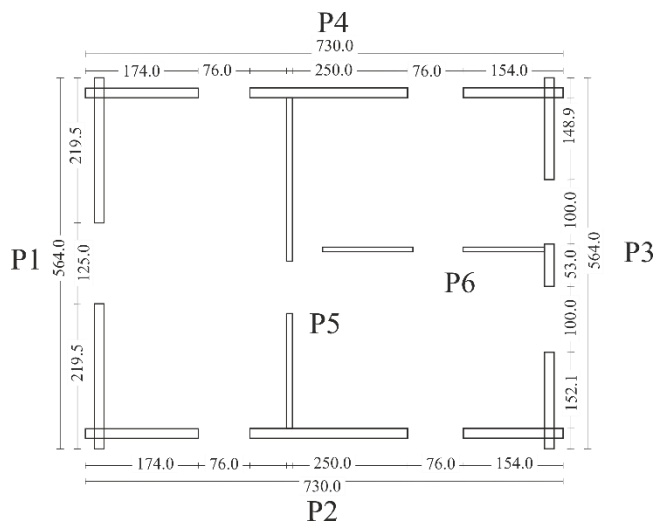


Figure 8. First and second floor plan

The roof structure is characterized by massive wooden rafters of cross-section 70x190mm. The rafters are inclined at an angle of 18°, over which OSB panels are nailed.

The ridge board has a cross-section of 120x200mm and is parallel to the longitudinal walls of the house. Grooves are provided at the locations where the transverse walls intersect the ridge board. The top ends of the rafters lie on the ridge board and are supported near their ends by the top logs of the longitudinal walls.

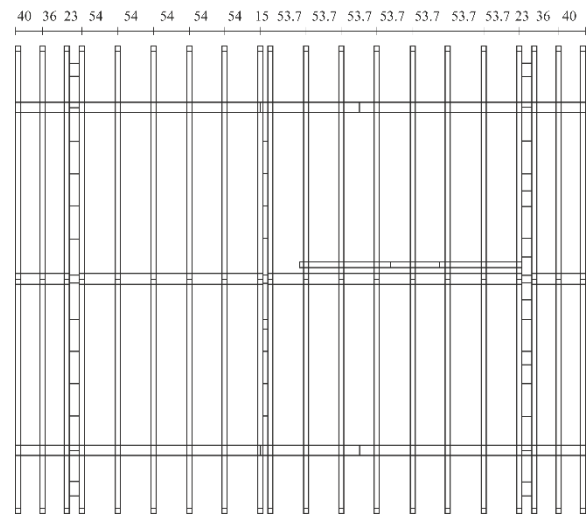


Figure 9. Roof plan

The logs used in the construction of the walls form a perfect fit with each other as they are shaped both at the top and bottom. The ends of the logs are notched to facilitate the intersection of the cross wall.

In the corner joints the presence of construction gaps of 1mm was accounted in order to simulate the real construction behaviour. The logs are made of glulam timber derived from Scots Pine trees (*Pinus sylvestris* L.) and belong to the C24 class of resistance according to (European committee for standardization 2003). The properties of the wood are listed in Table 1. The dimensions of the cross sections of the logs used in the outer walls and inner walls are 160x160mm and 80x160mm. The lamellas of each individual log are 40mm thick. The inner and outer walls are composed of two and four lamellas (SERIES 2013).

Table 1. Scots Pine wood, class C24 (SERIES, 2013)

Properties	Symbols	
Bending strength	$f_{m,k}$ [N/mm <sup>2</sup> ]	24
Tensile strength	$f_{t,90,k}$ [N/mm <sup>2</sup> ]	14
	$f_{t,0,k}$ [N/mm <sup>2</sup> ]	0.5
Compressive strength	$f_{c,90,k}$ [N/mm <sup>2</sup> ]	21
	$f_{c,0,k}$ [N/mm <sup>2</sup> ]	2.5
Modulus of Elasticity	$E_{0,mean}$ [N/mm <sup>2</sup> ]	11000
	$E_{90,mean}$ [N/mm <sup>2</sup> ]	370
Shear Modulus	$G_{mean}$ [N/mm <sup>2</sup> ]	690
Density	$\rho$ [kg/m <sup>3</sup> ]	530
Poisson's ratio	$\nu$	0.3

In the log walls, screws of 10x140mm are used around the openings and screws of 8x240mm are used near the joints of the cross walls.

The floor seismic weight is 60.7, 54.9 and 32.0kN for walls W1 to W3.

### 3.4 Case of study introduction: Modal-DBD design steps

The building has been analyzed independently in the two plan directions (X,Y). The Modal-DBD steps defined in section 2 are developed in both the X and Y direction analyses.

#### 3.4.1 Target Performance Level definition

The first step of Modal-DBD method requires to define the displacement limits for different hazard levels (Table 2). For each displacement level a Non-Exceedance (NE) probability has been assigned. The ASCE/SEI-7-16 (2016), prescriptions requires the following displacement targets:

Table 2. ASCE/SEI-7 Allowable Story Drift for structures other than masonry

Level	Performance Expectations	
	Exceedance probability	Drift limit
Level IO	50%/50 yr	0.5%
Level LS	10%/50 yr	1%
Level CP	2%/50 yr	2%

Currently, for timber structures, there aren't specific drift limits, in particular interstory drift level that reach a building up to collapse has not yet been universally agreed on.

Based on the evidences of experimental test find in lictérature, the limits presented in Table 3 for Blockhaus structures are too conservative.

For the Immediate Occupancy level has been chosen the limitation of interstorey drift in suggested in [§ 4.4.3.2(b)] of EC8 for buildings having ductile non-structural elements, corresponding to 0.75%.

For the Life Safety level, has been adopted the limit suggested in §12, Table 12.12.1 of ASCE 7-16 (2016), of 2.5% for structures other than masonry with four or less stories and risk category I or II.

Based on lictérature values of collapse displacements for Blockhouse structures, the drift of 3% has been incremented to 4% as the collapse prevention drift level (Table 3).

Table 3. Adopted drift limits for Blockhaus structures

Level	Performance Expectations	
	Exceedance probability	Drift limit
Level IO	50%/50 yr	0.75%
Level LS	10%/50 yr	2.5%
Level CP	2%/50 yr	4%

#### 3.4.2 Site choice and definition of seismic conditions

The building is designed for the site (Lat. 40.79, Long. -124.16) located in Eureka, California, assuming Site Class C (very dense soil and soft rock) (ASCE 7-16 soil classification).

The spectral acceleration parameters  $S_S$  and  $S_I$  are determined by the USGS seismic risk maps updated to 2014. These acceleration parameters refer to the maximum objective considered earthquake ( $MCE_R$ ), which for a specific area, is an earthquake that should occur once every 2475 years or so; that is, it has a 2% chance of being exceeded in 50 years.

The  $MCE_R$  spectral response acceleration parameters for short periods ( $S_{MS}$ ) and at 1s ( $S_{M1}$ ), adjusted for site class effects, shall be determined by Equations (6) and (7), respectively.

$$S_{MS} = F_a S_S \quad (4)$$

$$S_{M1} = F_v S_I \quad (5)$$

Where  $F_a$  and  $F_v$  are site coefficients defined in ASCE 7-16 §11.4. The values are represented in Table 4.

Table 4. Site Class parameters

Level	Exceedance probability	$S_S$ [g]	$S_I$ [g]	$F_a$	$F_v$	$S_{MS}$ [g]	$S_{M1}$ [g]
Level IO	50%/50 yr	0.82	0.32	1.2	1.5	0.98	0.75
Level LS	10%/50 yr	1.87	0.72	1.2	1.4	2.46	1.01
Level CP	2%/50 yr	2.81	1.09	1.2	1.4	3.37	1.52

Design earthquake spectral response (Figure 10) acceleration parameters at short periods,  $S_{DS}$ , and at 1-s periods,  $S_{D1}$ , shall be determined from Eqs. (8) and (9), respectively.

$$S_{DS} = \frac{2}{3} S_{MS} \quad (6)$$

$$S_{D1} = \frac{2}{3} S_{M1} \quad (7)$$

The design response spectrum curve is taken from the following equations:

For periods less than  $T_0$ , the design spectral response acceleration,  $S_a$ , shall be taken as given in Equation (4.51):

$$S_a = S_{DS} \left( 0.4 + 0.6 \frac{T}{T_0} \right) \quad (8)$$

For periods greater than or equal to  $T_0$  and less than or equal to  $T_S$ , the design spectral response acceleration,  $S_a$ , shall be taken as equal to  $S_{DS}$ .

For periods greater than  $T_S$  and less than or equal to  $T_L$ , the design spectral response acceleration,  $S_a$ , shall be taken as given in Equation (11):

$$S_a = \frac{S_{D1}}{T} \quad (9)$$

For periods greater than  $T_L$ ,  $S_a$  shall be taken as given in Equation (12):

$$S_a = \frac{S_{D1}T_L}{T^2} \quad (10)$$

where

$S_{DS}$  = the design spectral response acceleration parameter at short periods

$S_{D1}$  = the design spectral response acceleration parameter at a 1-s period

$T$  = the fundamental period of the structure, s

$T_0 = 0.2 (S_{D1}/S_{DS})$

$T_S = S_{D1}/S_{DS}$ , and

$T_L$  = long-period transition period(s) dependent on site.

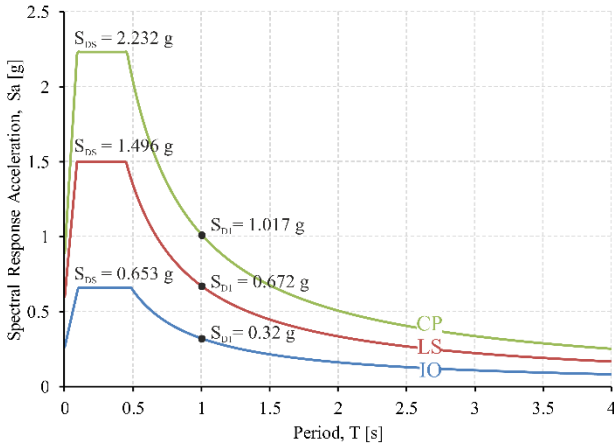


Figure 10. Design acceleration response spectra for Eureka, California.

### 3.4.3 Definition of equivalent mass and stiffness matrices

The base of the Modal-DBD is the development of a modal analysis to introduce the Equivalent Structure. The procedure consists in an equivalent linearization of a non-linear multigrade freedom system (MDOF) in which the story stiffness of the linear elastic MDOF system is estimated with a rigidity equivalent at the target inter-story drift. The X-direction and Y-direction were analyzed independently. The natural frequencies,  $\omega_n$  and mode shape  $\varphi_n$ , are determined by solving the following eigenvalue problem:

$$\left[ K - \omega_n^2 M \right] \varphi_{jn} = 0 \quad (11)$$

where  $K$  and  $M$  are the stiffness and mass matrices. The mass matrix is a diagonal matrix,

$$M = m \begin{bmatrix} 1 & 0 & 0 \\ 0 & \beta_{m2} & 0 \\ 0 & 0 & \beta_{m3} \end{bmatrix} \quad (12)$$

where  $m$  is the total lumped mass for first floor and  $\beta_{mj}$  is the  $j$ -th floor mass ratio (relative to the first floor). The stiffness matrix is given by,

$$K = k \begin{bmatrix} 1 + \beta_{k2} & -\beta_{k2} & 0 \\ -\beta_{k2} & \beta_{k2} + \beta_{k3} & -\beta_{k3} \\ 0 & -\beta_{k3} & \beta_{k3} \end{bmatrix} \quad (13)$$

The stiffness was considered proportional to each wall length, net to openings.

The natural frequencies,  $\omega_n$  [rad/sec], and periods,  $T_n$  [s], for the  $n$ -th mode are given by,

$$\omega_n = \alpha_n \sqrt{\frac{k}{m}} \quad (14)$$

$$T_n = \frac{2\pi}{\alpha_n \sqrt{\frac{k}{m}}} = \frac{\bar{T}}{\alpha_n} \quad (15)$$

### 3.4.4 Perform the Normalized modal analysis

An eigenvalue analysis for the Blockhaus system, was carried on; the modal participation factor ( $\Gamma_n$ ) for the  $n$ -th mode was calculated as:

$$\Gamma_n = \frac{\sum_{j=1}^{N_{floor}} \beta_{mj} \varphi_{jn}}{\sum_{j=1}^{N_{floor}} \beta_{mj} (\varphi_{jn})^2} \quad (16)$$

Where  $N_{floor}$  represent the total number of floors in the structure, in the case of study is equal to 3. In order to measure the contribution of each mode to  $\Gamma_n$ , the the inter-story drift factor  $\gamma_{jn}$ , independent from the normalization, is introduced:

$$\gamma_{jn} = \Gamma_n (\varphi_{jn} - \varphi_{j-1,n}) \quad (17)$$

### 3.4.5 Design the inter-story drift spectra

A conversion of the design acceleration response spectrum into a displacement response spectrum,  $S_d$ , is first performed:

$$S_d(T) = \left( \frac{T}{2\pi} \right)^2 S_a(T) \quad (18)$$

Modal expansion and combination procedures are incorporated into a single equation (SRSS modal combination rule) that can be used to generate the inter-story drift spectra:

$$\Delta_j(\bar{T}) = \frac{1}{H_j} \sqrt{\sum_n \left[ \gamma_{jn} \left( \frac{\bar{T}}{\alpha_n 2\pi} \right)^2 S_a \left( \frac{\bar{T}}{\alpha_n} \right) \right]^2} \quad (19)$$

### 3.4.6 Definition of weakest floor and equivalent stiffness

By plotting the the inter-story drift spectra for each plane together on a single figure, the weakest floor is the first that reaches the limit drift of Section 3.4.1. Defined the period  $\bar{T} = \bar{T}_{req}$ , the other floor drift can be defined.

The required equivalent rigidity for each floor,  $(k_{eq})_j$ , can be calculated using the following equation once the required equivalent period has been determined:

$$(K_{eq})_j = \left( \frac{2\pi}{T_{req}} \right)^2 m \beta_{kj} \quad (20)$$

where  $m$  and  $\beta_{kj}$  are previously defined.

### 3.4.7 FE model of log-walls to define the backbone parameters

In order to define the backbone parameters, the entire log-walls named P1, P2, P3 and P4 have been respectively divided into three parts, named GF (Ground Floor), FF (First Floor) and SF (Second Floor). Each part has been modelled as full scale log-wall via FE, using the software Abaqus/Explicit (Dassault Systèmes 2015).

At first, to guarantee the consistency of the log-walls FE models, it has been reproduced a FE model having the same geometrical features of the one presented in experimental test conducted by Bedon et. al, (2015). The model has been realized by assembling different parts. The general longitudinal log, consists on 3D continuous deformable regular element, 160 x 160 mm cross section and different length, the half longitudinal log has the same length and a cross section 160 x 160mm.

The transversal walls were also represented as overlapping logs of with the same cross section of the longitudinal one and smaller length 1m. The top steel beam was also accounted.

Three different materials have been considered; steel in plate and cable is

considerated as isotropic, linear elastic ( $\rho_s = 7,500 \text{ kg/m}^3$ ,  $E_s = 130 \text{ GPa}$ , and  $\nu_s = 0.32$ ) (Eurocode 3 (2004b)). For the steel hollow reinforcements a structural steel S275 ( $\rho_s = 7,850 \text{ kg/m}^3$ ,  $E_s = 210 \text{ GPa}$ , and  $\nu_s = 0.3$ ) has been considerate. C24 Scot Pine has been modelled as orthotropic, elastoplastic material with resistance parameters available in the Table .

The contact is assessed as a boundary non-linearity. General contact interactions were automatically detected between overlapping logs, along their entire length, and between main logs and orthogonal logs based on the nominal geometry of joints.

The typical finite-element (FE) model consisted of 8-node, linear brick, solid elements with reduced integration (C3D8R). The vertical 10mm-diameters cable was modelled using truss elements (T3D2 type).

The vertical compression load was described by means of a uniformly distributed, constant vertical pressure applied to the upper surface of the steel beam, the amount of load was defined for each log-wall. An horizontal in-plane lateral displacement was applied to the edge surface of the steel beam as a uniform, quasi-static, linearly increasing time-varying displacement BC. The maximum displacement was set equal to 200mm for each wall.

Geometrical imperfections were taken into account in ABAQUS numerical model, including gaps, see (Bedon et al. 2015a).

In Figure 11 and 12 the contour plot displacement for two representative log-wall is shown.

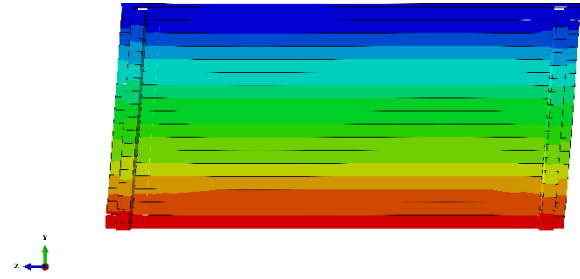


Figure 11. Abaqus lateral displacement contour plot for log-wall P3 Ground Floor

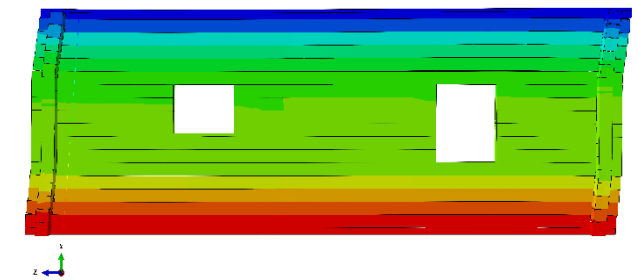


Figure 12. Abaqus lateral displacement contour plot for log-wall P4 Ground Floor

The CASHEW model (Foschi 1974) was thus adopted in this study.

In the CASHEW model, the load displacement behavior at the top of the wall is modeled using a non-linear SDOF spring. Only five parameters of the backbone curve are used in the Modal-DBD procedure, and the envelope response of a wooden shearwall follows Eq.(23):

$$F_b(\delta) = \begin{cases} \left[ 1 - e^{-\frac{K_0 \delta}{F_0}} \right] (r_1 K_0 \delta + F_0) & \text{for } \delta \leq \delta_u \\ F_u + r_2 K_0 (\delta - \delta_u) & \text{for } \delta > \delta_u \end{cases} \quad (21)$$

Where  $K_0$  is the initial tangent stiffness of the backbone curve,  $F_b$ , represents the restoring force,  $F_u$  is the maximum load-carrying capacity associated with the last displacement,  $\delta_u$ . (see Figure 13)

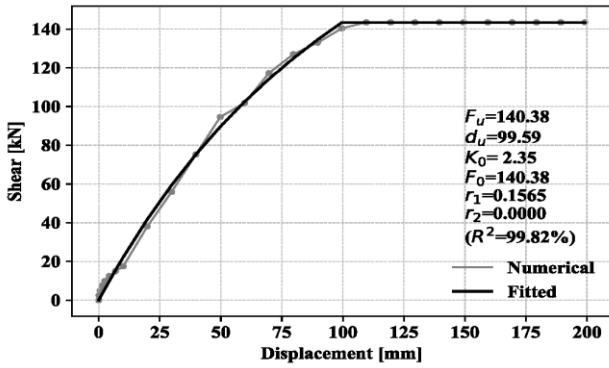


Figure 13. Abaqus lateral displacement contour plot for log-wall P4 Ground Floor

### 3.4.8 Equivalent linearization of NL Backbone Curve

The shearwall energy is defined as:

$$E_{NL} = \int_0^{\delta_i} F_b(\delta) d\delta \quad (22)$$

Where  $F_b(\delta)$  has been previously defined in Equation (23). The energy stored in the equivalent elastic system is:

$$E_L = \frac{1}{2} k_{eq} \delta_i^2 \quad (23)$$

And so the equivalent elastic stiffness  $k_{eq}$  is:

$$k_{eq} = \frac{2E_{NL}}{\delta_i^2} \quad (24)$$

### 3.4.9 Shear and uplift force estimation

The story shear force,  $V_j$  and base shear (shear force of the first story) can be determined by summing the actual shearwall backbone forces ( $F_b$  given by Eq (4.54)) at the target drift profile:

$$V_j = \sum_{walls} \begin{cases} F_b(\Delta_j(\bar{T}_{req})h) & \text{for } \Delta_j(\bar{T}_{req})h < \delta_u \\ F_u & \text{for } \Delta_j(\bar{T}_{req})h \geq \delta_u \end{cases} \quad (25)$$

The maximum uplift force,  $F_{up}$ , developed on the end studs can be estimated on the basis of the height-to-width ratio of the full-height wall segment:

$$F_{up} = \frac{h}{\sum_{walls} B} V_j \quad (26)$$

where  $B$  is the width of the single shearwall and  $h$  the relative height.

### 3.4.10 Modal-DBD application

The mass ratios,  $\beta_m$ , have been obtained by the analysis of acting loads. The mass ratios (relative to the first floor) are 1.0, 0.90, and 0.53 for the first, second, and third floors, respectively.

The initial  $\beta_k$  have been estimated by calculating the total available shearwall length, in the direction considered, for each story in accordance with (Folz and Filiatrault 2002).

The results for the normalized modal analysis for the Y-direction are shown in Figure 14.

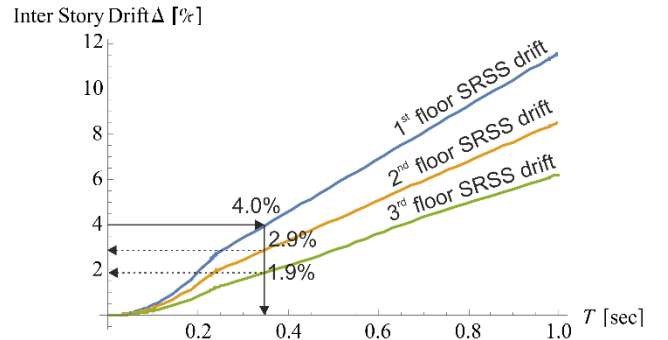


Figure 14. Direct displacement design for the CP performance level in Y-direction

At the CP level, the actual stiffness ratios at the increased for the first story from 1.71 to 2.09, for the second from 1.35 to 2.19 and at least, for the third from 1.35 to 3.22. As a final step, another normalized modal analysis is performed (using the actual values of  $\beta_k$ ) to determine new story drift estimates and required equivalent stiffnesses. The new drift predictions are below the CP drift limit (i.e., 4%) and the required equivalent stiffnesses are lower than the actual equivalent stiffnesses provided. Thus, the design meets the CP performance requirements. The stiffness of the actual lateral force resisting system, parallel to the east and west walls, is about 27~28% higher than the minimum required stiffness. This verification process completes the DDD procedure for one performance level.

The actual stiffness ratios accounted for the design verification in CP level, were considered as initial stiffness parameters for the LS level analysis, a similar procedure previously described was applied to check the LS drift limit (i.e., 2.5%), it results that the shearwalls parallel to the east and west walls stiffness, is about 33~33% higher than the minimum required stiffness.

At least the IO level was analyzed, but the drift limitation accounted for 0.75% proved to be too restrictive. The stiffness of the shearwalls parallel to the east and west walls, is about 16% smaller than the minimum required stiffness. The same situation occurs at the IO level analysis in Y-direction; in this case the stiffness provided by the resisting walls is slightly smaller than the required (3%).

The shear force for each floor in X and Y-direction are shown below in Table 5 and 6 respectively:

Table 5. Shear force in X-direction

Floor	Performance level		
	CP	LS	IO
	Story Shear [KN]		
1	212	182	73
2	193	137	53
3	91	58	23

Table 6. Shear force in Y-direction

Floor	Performance level		
	CP	LS	IO
	Story Shear [KN]		
1	286	220	84
2	235	169	63
3	157	76	30

#### 4 CONCLUSIONS

A Modal- displacement-based seismic design procedure for multi-story Blockhaus structure of regular shape with relatively symmetric plan and rigid diaphragms (i.e., no torsional effects) has been presented. Inter-story drift is assumed as a key design parameter to predictor of damage in timber structures. The backbone parameters have been evaluated by FE procedure and curve fitting.

The CP and LS level are widely verified but has been highlight that the fixed drift limit equal to 0.75% for IO is too conservative and is not verified cause the Blockhaus shearwall geometrical features (in particular the small mounting gaps in the corner joints). In the future non-linear static analyses will be carried out to verify the Modal-DBD procedure.

#### REFERENCES

- ASCE 41-17, 2017. Seismic Evaluation and Retrofit of Existing Buildings.
- ASCE 7-16, 2016. Minimum Design Loads and Associated Criteria for Buildings and Other Structures.
- Bedon, C., Fragiaco, M., Amadio, C., & Sadoch, C., 2014. Experimental study and numerical investigation of Blockhaus shear walls subjected to in-plane seismic loads. *Journal of Structural Engineering*, **141**.
- Bedon, C., Rinaldin, G., & Fragiaco, M., 2015. "Non-linear modelling of the in-plane seismic behaviour of timber Blockhaus logwalls. *Engineering Structures*, **91**(5), 112-124.
- Bedon, Rinaldin, G., Fragiaco, M., & Noè, S., 2016. Finite element assessment of the seismic performance of three dimensional Blockhaus buildings. *World Conference on Timber Engineering -WCTE 2016*. Vienna, AU.
- Bolvardi, V., Pei, S., Lindt, J. v., & Dolan, J., 2018. Direct displacement design of tall cross laminated timber platform buildings with inter-story isolation. *Engineering Structures* **167**, 740-749.
- Branco, J., & Araújo, J. P., 2010. Lateral resistance of log timber walls subjected to horizontal loads. *Proceedings of WCTE 2010*.
- CEN, E. C., 2004. EN 1998-1:2004, Eurocode 8, Design of structures for earthquake resistance, part 1: general rules, seismic actions and rules for buildings. Brussels, The Netherlands: CEN.
- Dassault Systèmes., 2015. *Abaqus, F.E.A. V. 6.12*
- Fajfar, P., & Gasperic, P., 1996. The N2 method for the seismic damage analysis of RC buildings. *Earthquake Engineering Structures* **25**(1), 31-46.
- Foliente, G., 1998. Design of timber structures subjected to extreme loads. *Progress in Structural Engineering and Materials*, 236-244.
- Folz, B., & Filiatrault, A., 2001. Cyclic analysis of wood shear walls. *Journal of Structural Engineering ASCE* **127**, 433-441.
- Foschi, R. O., 1974. Load-slip Characteristics of Nails. *Wood Science*, **7**(1), 69-76.
- Frangiaco, M., Riu, R., & Scotti, R., 2015. Can structural timber forest short procurement chains with Mediterranean Forest? A reseache case in Sardinia. *SEEFOR South-East European Forestry*.
- Gkimprxis, A., Tubaldi, E., & Douglas, J., 2019. Comparison of methods to develop risk-targeted seismic design maps. *Bulletin of Earthquake Engineering*, **17**, 3727-3752.
- Grossi, P., Sartori, T., Giongo, I., & Tomasi, R., 2016. Analysis of timber log-house construction system via experimental testing and analytical modelling. *Construction and Building Materials*, **102**(2), 1127-1144.
- Gupta, A. K., & Kuo, G. P., 1985. Behavior of Wood-framed Shear Walls. *ASCE Journal of Structural Engineering*, **111**(8), 1722-1733.
- ICC., 2018. *International Building Code*.
- Loss, C., Tannert, T., & Tesfamariam, S., 2018. State-of-the-art review of displacement-based seismic design of

- timber. *Construction and Building Materials*, **191**, 481-497.
- Pang, W. C., & Rosowsky, D.V., 2009. Direct displacement procedure for performance-based seismic design of mid-rise wood-framed structures. *Earthquake Spectra* **25**, 583-605.
- Priestley, M. J., Calvi, G. M., & Kowalsky, M. J., 2007. Displacement-Based Seismic Design of Structures. *IUSS Press, Pavia*.
- Sciomenta, M., Bedon, C., Fragiaco, M., & Luongo, A., 2018. Shear Performance Assessment of Timber Log-House Walls under In-Plane Lateral Loads via Numerical and Analytical Modelling. *Buildings*, **8**(8), 99.
- SERIES, 2013. Seismic engineering research infrastructures for european synergies. *Seismic performance of multi-storey timber buildings - Final Report*.